Journal of Physics: Conference Series **318** (2011) 052029 doi:10.1088/1742-6596/318/5/052029

Compressive and extensive strain along gradient trajectories

Markus Gampert[1], Jens Henrik Goebbert[1], Philip Schaefer[1], Michael Gauding[1], Norbert Peters[1], Fettah Aldudak[2] & Martin Oberlack[2]

[1]Institut für Technische Verbrennung, RWTH Aachen, Germany
[2]Fachgebiet für Strömungsdynamik, Technische Universität Darmstadt, Germany

E-mail: m.gampert@itv.rwth-aachen.de

Abstract. Based on direct numerical simulations of forced turbulence, shear turbulence, decaying turbulence, a turbulent channel flow as well as a Kolmogorov flow with Taylor based Reynolds numbers Re_λ between 69 and 295, the normalized probability density function of the length distribution $\tilde{P}(\tilde{l})$ of dissipation elements, the conditional mean scalar difference $< \Delta k \mid l >$ at the extreme points as well as the scaling of the two-point velocity difference along gradient trajectories $< \Delta u_n >$ are studied. Using the field of the instantanous turbulent kinetic energy k as a scalar, we find a good agreement between the model equation for $\tilde{P}(\tilde{l})$ as proposed by Wang and Peters (2008) and the results obtained in the different DNS cases. This confirms the independance of the model solution from both, the Reynolds number and the type of turbulent flow, so that it can be considered universally valid. In addition, we show a 2/3 scaling for the mean conditional scalar difference. In the second part of the paper, we examine the scaling of the conditional two-point velocity difference along gradient trajectories. In particular, we compare the linear s/τ scaling, where τ denotes an integral time scale and s the separation arclength along a gradient trajectory in the inertial range as derived by Wang (2009) with the $s \cdot a_\infty$ scaling, where a_∞ denotes the asymtotic value of the conditional mean strain rate of large dissipation elements.

1. Introduction

One of the many approaches in turbulence research is to study geometrical structures in terms of critical points in the flow field. Gibson (1968) analyzed the behaviour of zero gradient points and minimal gradient surfaces in turbulent scalar fields. Based on the extreme points of turbulent scalar fields, i.e. points of vanishing scalar gradient, Wang & Peters (2006, 2008) developed the theory of dissipation elements, which arise as natural geometries in turbulent scalar fields, when these are analyzed by means of gradient trajectories. Starting from every grid point, trajectories along the ascending and descending gradient direction can be calculated, which inevitably end at extreme points. All points that share the same two ending points define a finite volume which is called a dissipation element. These elements are parameterized by two values, namely the linear length l between and the scalar difference Δk at the extreme points, where k is the scalar to be used in the present paper. Based on this theory, space-filling elements are identified, which allow the reconstruction of statistical properties of the field as a whole in terms of conditional statistics within the elements.

From the definition follows that the temporal evolution of dissipation elemenets in turbulent fields is inherently connected to the evolution of their ending points, which are separated by a mean linear distance l_m of the order of the Taylor microscale λ, see Wang & Peters (2006). While strain and diffusion lead to a continuous distortion of an element as a whole, the creation or annihilation of extreme points leads to their abrupt formation or dissappearance. These different effects have successfully been considered in a modelled evolution equation for the probability density function (pdf) for the length distribution $P(l)$ of dissipation elements, which in its normalized form $\tilde{P}(\tilde{l})$ is assumed to be independent of both, the Reynolds number and the type of turbulent flow. In this equation two parameters appear, cf. Wang & Peters (2008), which can be identified as a splitting respectively attachment frequency of the elements and thus indirectly correspond to the life time of extreme points, see Schaefer *et al.* (2009, 2010*b*) for further details. A third important parameter employed in Wang & Peters (2008) for the description of the pdf of the length distribution, is the normalized rate of strain $\tilde{a}$. The strain rate is defined as the difference of the velocity at the ending points, projected in direction of the connecting line between the two extreme points. It will be shown below that there is a linear scaling of the mean absolute value of the velocity difference with the curvilinear distance along gradient trajectories for large elements.

The basis for this scaling is a paper by Wang (2009), who studied the two-point correlation of scalar gradients along gradient trajectories. Starting from the governing equation for the passive scalar, a decorrelation assumption for the product of two-point scalar gradients and the velocity difference in the triple correlation term is used to derive a positive linear scaling of the velocity difference with curvilinear separation distance along the trajectory s and the inverse of the integral time scale τ. Furthermore, Wang shows that this result is in good agreement with data obtained from direct numerical simulations (DNS) of homogenous shear turbulence. It is argued that due to a conditioning of the statistics on gradient trajectories, regions of large extensive strain, which smooth the scalar field, are preferentially extracted, thereby allowing a gradient trajectory to extend over large distances. For relatively short distances in the viscous range however, with $s < \lambda$, no analytic expression for the scaling of the velocity difference has been derived so far. Based on an argument involving the curvature term, which arises in the derivation of the governing equation along trajectories, a negative value for the velocity difference is qualitatively concluded by Wang (2009).

The intention of the present paper is two-fold. In a first step, we will examine the validity of the model for the pdf of the linear element length as derived by Wang & Peters (2008) as well as the Kolmogorov scaling of the conditional scalar difference for different types of turbulent flows. In a second step, the universality of the two-point velocity difference $< \Delta u_n >$ along gradient trajectories is analyzed. To this end, we examine the validity of Wang's scaling for long trajectories.

In contrast to previous work, all gradient trajectory and dissipation element analysis presented in this paper is based on the field of the instantaneous turbulent kinetic energy k. This appears reasonable as it allows a direct interaction between the underlying velocity field and the examined scalar field as well as the evaluation of the energy budget along gradient trajectories. In addition, the field of the turbulent kinetic energy can easily be evaluated from investigations of the three-dimensional velocity field and consequently simplifies an experimental verification of the theoretical results, see for instance Schaefer *et al.* (2010*a*).

As numerical test cases, DNS of various turbulent flows have been performed. Details of the different flow setups are given at the beginning of chapter 2. Before, we present the results of the dissipation element analysis. The two-point velocity difference along gradient trajectories is discussed in chapter 3, and a conclusion is drawn in chapter 5.

2. Dissipation element analysis

Direct numerical simulations of six different types of turbulent flows, namely of homogenous shear turbulence (case 1 and 2), homogeneous isotropic forced turbulence (case 3), homogeneous isotropic decaying turbulence (case 4), a channel flow (case 5) as well as a Kolmogorov flow (case 6) were performed. Cases 1-4 and case 6 were run on the JUGENE Supercomputer of the Research Center Jülich using up to 16,384 CPU's for the calculations and case 5 on the HHLR Darmstadt. In all cases the Kolmogorov length $\eta = (\nu^3/\varepsilon)^{1/4}$ was resolved, which is particularly important for dissipation element analysis. Taylor based Reynolds numbers $Re_\lambda = u'\lambda/\nu$ between 69 and 295 have been investigated, with the Taylor microscale $\lambda = \sqrt{10\nu k/\varepsilon}$ and the turbulence intensity $u' = \sqrt{2k/3}$.

An overview of the numerical parameters and selected mean quantities is given in table 1. Note, that the values for case 5 originate from the channels core region, while for case 6 all y-dependant quantities have been averaged over the inhomogenous direction.

The motivation for dissipation elements is the reconstruction of the entire three-dimensional scalar field by means of an adequate description of an element's characteristics. The corresponding joint probability density function (jpdf) $P(l, \Delta k)$ is expected to contain most of the information needed for a statistical reconstruction. Based on a trajectory search algorithm, the field of the turbulent kinetic energy has been analyzed for the different DNS cases and the resulting joint pdf for case 1 is shown in figure 1 (to relate the values of l and Δk given in this figure to other characteristic flow quantities see table 1). In this illustration, different physical effects are illustrated. Besides a distinct maximum, one observes a decrease at the origin, corresponding to the annihilation of small elements due to molecular diffusion. The region in the upper right hand area of the jpdf is dominated by extensive strain, as large elements are exposed to large velocity differences.

Additionally, a dotted line corresponding to the conditional mean $< \Delta k \mid l >$ is included in figure 1(left), revealing a scaling with Kolmogorov's 2/3. This finding will be discussed in more detail later, see figure 4. However, the spread of the jpdf around this mean value is obviously not symmetric and can therefore not be described by a Gaussian distribution, see figure 1(right).

The jpdf can be described by a model equation. Based on Bayes theorem, it is decomposed into a marginal pdf $P(l)$ of the linear distance and a conditional pdf $P(\Delta k \mid l)$ of the scalar difference, yielding

Table 1. Parameters of the different DNS cases.

DNS case	1	2	3	4	5	6
Flow type	Shear	Shear	Forced	Decaying	Channel	Kolmogorov
No. of grid cells	2048^3	1024^3	1024^3	1024^3	$512\times257\times256$	1024^3
Reynolds number Re_λ	295	139	144	71	69	188
viscosity ν	$9\cdot10^{-4}$	$2\cdot10^{-3}$	$2.8\cdot10^{-3}$	$5\cdot10^{-4}$	$1.5\cdot10^{-5}$	$2.5\cdot10^{-4}$
kinetic energy k	3.510	1.925	3.210	0.049	$3.8\cdot10^{-5}$	0.115
dissipation ε	1.160	0.640	1.190	0.001	$3.5\cdot10^{-7}$	0.010
Kolmogorov scale η	0.005	0.011	0.017	0.010	0.010	0.006
Taylor length λ	0.165	0.245	0.275	0.135	0.134	0.170
resolution $\Delta x/\eta$	0.610	0.558	0.361	0.610	0.993	0.970
mean linear distance l_m	0.198	0.356	0.422	0.281	0.266	0.245
l_m/λ	1.200	1.453	1.536	2.081	1.988	1.441

$$P(l, \Delta k) = P(l)\ P(\Delta k \mid l), \tag{1}$$

where the marginal pdf $P(l)$ is defined by

$$P(l) = \int_0^\infty P(\Delta k, l) d\Delta k. \tag{2}$$

For this pdf in its normalized form $\tilde{P}(\tilde{l})$, with $\tilde{P} = P\ l_m$ and $\tilde{l} = l/l_m$, the following model equation was derived by Wang & Peters (2008)

$$\frac{\partial \tilde{P}(\tilde{l}, \tilde{t})}{\partial \tilde{t}} + \frac{\partial}{\partial \tilde{l}}(\tilde{P}(\tilde{l}, \tilde{t})[\tilde{v}_D(\tilde{l}) + \tilde{a}(\tilde{l})\tilde{l}]) = \Lambda_s \int_{\tilde{l}}^\infty \tilde{P}(\tilde{z}, \tilde{t}) d\tilde{z} - \Lambda_a \tilde{l} \tilde{P}(\tilde{l}, \tilde{t}). \tag{3}$$

In this equation, $\tilde{a}$ represents the conditional mean strain rate a of the elements of length l

$$a = \frac{< \Delta u_n \mid l >}{l}. \tag{4}$$

normalized by its asymptotic value a_∞, which is approached for $l \to \infty$.

In eq. 4, Δu_n denotes the velocity difference between an element's maximum and minimum projected in trajectory direction.

The results for $a(l)$ have been calculated for all DNS cases and its conditional mean is compared to the model proposed by Wang & Peters (2008),

$$a = a_\infty \Big(1 - \frac{0.4}{\tilde{l} + 0.1}\Big), \tag{5}$$

where the value of a_∞ was also obtained from the DNS.

Figure 2 depicts the comparison of eq. 5 with DNS data. One observes a qualitatively similar shape for all DNS cases, as well as a good agreement between DNS data and model equation. The value of a_∞ ranges from 0.68 for the Kolmogorov flow to 4.10 for the shear turbulence.

Finally, $\widetilde{v_D}$, where

$$\widetilde{v_D} = v_D/(l_m\ a_\infty) = -4D/l \left(c\ \tilde{l}\ exp(-\tilde{l})\right)/(l_m\ a_\infty), \tag{6}$$

denotes the normalized drift velocity due to molecular diffusion in eq. 3 and is responsible for the linear decrease of $\tilde{P}(\tilde{l}, t)$ for $\tilde{l} \to 0$ as will be shown below. The constant c in eq. 6 is determined from the condition that the total length of the array must not change, cf. Wang & Peters (2008), and D is the molecular diffusion coefficient. In addition in eq. 3 the two non-dimensionalized

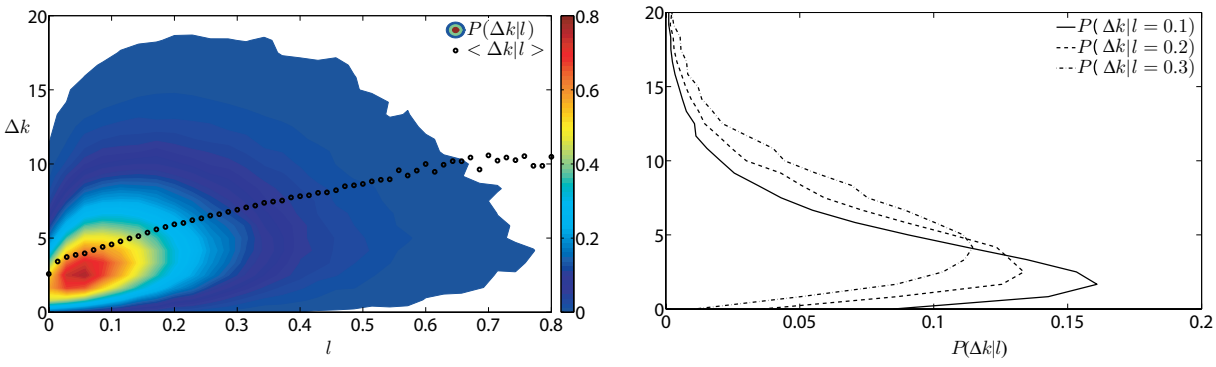

Figure 1. Joint probability density function $P(l, \Delta k)$ of case 1.

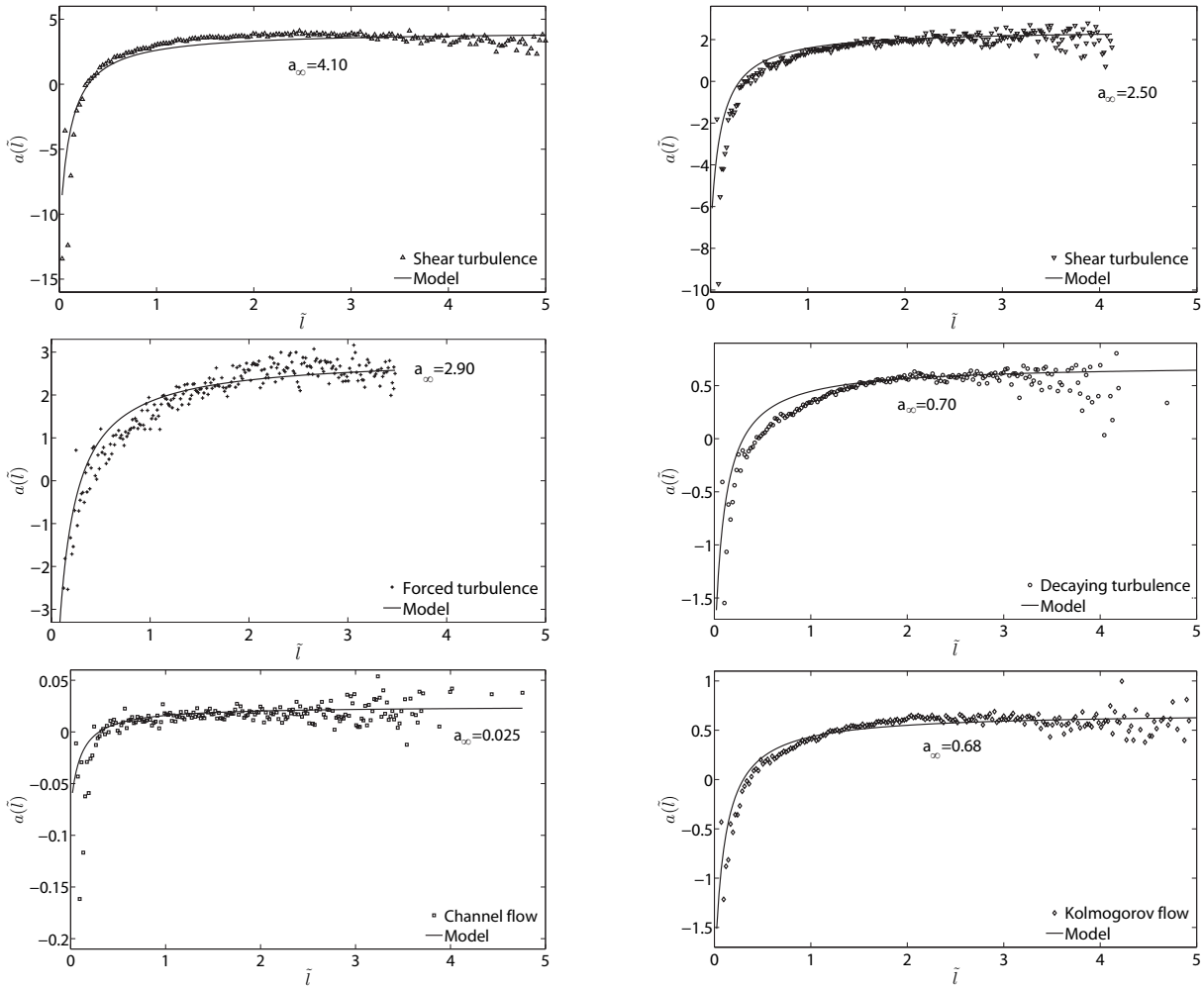

Figure 2. Comparison of conditional strain rate $a(\tilde{l})$ from model equation and DNS.

numbers Λ_s and Λ_a appear. These describe the splitting (respectively reconnection) of larger (smaller) elements into smaller (larger) ones and are determined from the normalization and the first moment during the solution of the equation as eigenvalues of the problem, cf. Schaefer *et al.* (2009). Eq. 3 can be solved numerically yielding the steady solution depicted by the solid curve in figure 3.

Furthermore, the results for the normalized pdf of the length distribution obtained from the different DNS cases are shown. One observes a very good agreement with the model solution. Slight differences can be identified in cases 4 and 6, where the model marginally underpredicts the maximal value of the pdf. The linear increase at the origin as well as the exponential tail however, see especially the log-in insets, follow more or less closely the predicted solution. For cases 1 and 5, the location and the overall shape of the pdf are tilted slightly to the left, resulting in a small deviation from the model, though the branches left and rigth from the maximum qualitatively agree nicely. (Note again that all data presented for case 5 here and in the following just stems from an evaluation in the core region of the channel.) However, deviations in the exponential tails (see the slopes of the pdf in the insets) of the pdf are hard to interpret due to the limited number of sample points. Nevertheless, figure 3 illustrates that the equation for $\tilde{P}(\tilde{l})$ seems not to be a function of the Reynolds number as the values of R_λ vary from 69 for the case of decaying turbulence to 295 for the shear turbulence. Overall, no conclusive influences due to the

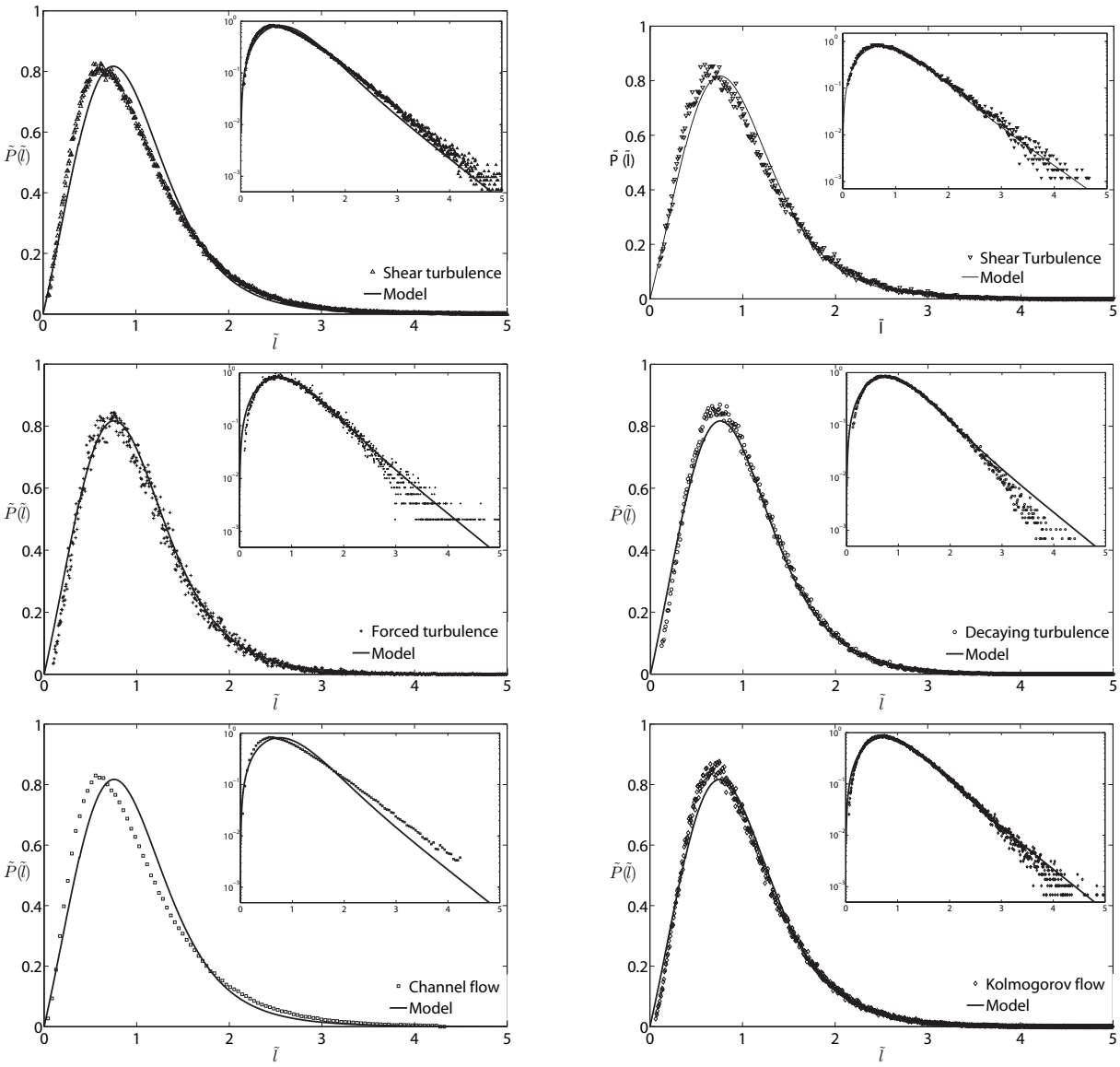

Figure 3. Comparison of normalized marginal pdf $\tilde{P}(\tilde{l})$ from model equation and DNS.

Reynolds number or based on the type of turbulent flow can be identified, so that the shape of the non-dimensional marginal pdf $\tilde{P}(\tilde{l})$ and its model equation may be considered independent from inhomogeneities and anisotropies, a finding which is illustrated in particular by the good agreement between the model and the Kolmogorov flow.

For the second term in eq. 1, the conditional pdf of Δk, no conclusive model equation was derived so far. In a first step, we will therefore analyze the conditional mean of Δk conditioned on the length of the respective dissipation element, defined by

$$< \Delta k \mid l >= \int_0^\infty \Delta k P(\Delta k \mid l)\, d\Delta k. \tag{7}$$

In unconditional statistics the first moment is equal to zero. For statistics based on gradient trajectories however, this is not the case, as the value of the turbulent kinetic energy increases per definition monotonically along a trajectory from the minimum to the maximum point.

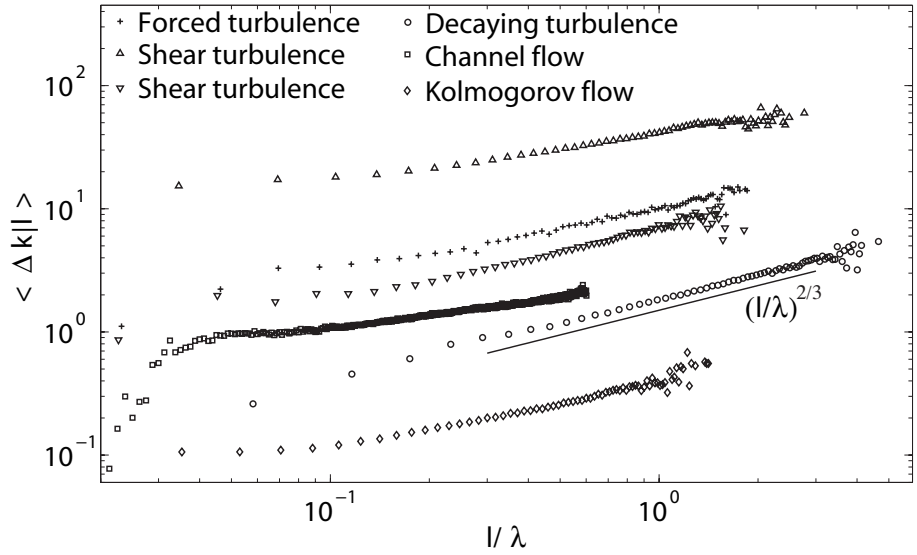

Figure 4. Conditional mean scalar difference $< \Delta k \mid l >$.

Consequently, we will study the first order conditional moment to examine its scaling. In Wang & Peters (2006, 2008) and Schaefer *et al.* (2010*c*) this conditional difference based on various scalar fields, such as for instance a passive scalar ϕ or the instantanous dissipation ε, was found to scale with Kolmogorov's 1/3 exponential dependance. In the present case for k however, one expects a scaling with 2/3 based on dimensional grounds. For the different DNS cases presented in chapter two, the results for $< \Delta k \mid l >$ are shown in figure 4.

One observes different absolute values for the difference of the instantanous turbulent kinetic energy between the extreme points of a dissipation element conditioned on its length (Note: for a better graphical illustration the channel flow data (case 5) has been shifted by four orders of magnitude, the shear flow data (case 1) has been multiplied by 5 and the decaying flow data (case 6) has been multiplied by 5). The symbols of the different DNS cases included in figure 4 however, show a scaling with 2/3 as indicated by the solid line with a slope of 2/3, which is more or less accurate for the different flow types. The best agreement is obtained in the case of decaying turbulence, while for example in shear turbulence a less pronounced 2/3 scaling is observed. In addition, it is obvious that Kolmogorov's scaling is also valid for dissipation element analysis based on the channel flow and the Kolmogorov flow, which are inhomogeneous and anisotropic flows.

3. Scaling of the velocity difference along gradient trajectories

In the course of this chapter, we will study the velocity difference at two points along gradient trajectories, motivated by the findings shown in figure 2. Conditioning on dissipation elements and more specifically on points along one trajectory, introduces major differences as compared to standard statistics in cartesian correlation space. Due to the limitation of the two-point statistics on points on the same trajectory only the correlation of specific points is studied. The conditional statistics along gradient trajectories also introduces differences with respect to the correlation coordinate. In contrast to statistics in correlation space of a cartesian grid, where the correlation coordinate usually denotes the linear distance between the two points under consideration, the correlation coordinate s is defined as the curvilinear distance of the two points along their trajectory. This obviously also introduces a flow dependant restriction

to the length of the new correlation coordinate as the mean distance of two points is the one between a maximum and a minimum point, which is of the order of the Taylor scale, as discussed in the previous chapter in the context of the dissipation element length and its pdf.

Compared to statistics in cartesian coordinates caution has to be exercised when the concepts of isotropy and homogeneity are used. In homogenous turbulence, the mean of the fluctuating component of the instantaneous velocity is by definition equal to zero. The velocity along trajectories u_n, however, is projected in trajectory direction $\mathbf{n}$, and therefore time and space dependent, yielding $u_n = \mathbf{u} \cdot \mathbf{n}$. The result of this product is a scalar, whose mean value is not by definition equal to zero. This difference also arises, when the first conditional moment is studied, which is of particular interest for the current work in trajectory coordinates, while it is equal to zero in the cartesian system.

In the following, we will study the scaling of the conditioned mean velocity increment $< \Delta u_n >$ along gradient trajectories . Based on the governing equation for a passive scalar ϕ in gradient coordinates, a relation for the inertial range was derived by Wang (2009). Neglecting the viscous term and assuming a decorrelation of the velocity difference from the two-point correlation of the scalar gradient, it is concluded that

$$< \Delta u_n > \propto s/\tau, \tag{8}$$

where the integral time scale is defined as $\tau = k/\varepsilon$. As this proportionality has only been validated by Wang (2009) and Wang & Peters (2011) for homogenous shear turbulence, we will examine its validity in the following for other flows.

In figure 5, the non-dimensional product $< \Delta u_n > (\tau/\lambda)$ is shown as a function of s/λ. In this figure the Taylor scale is used for the normalization rather than the Kolmogorov or an integral scale, as it is the representative length scale for gradient trajectories. One observes that both, the normalized velocity difference and the slope for all DNS cases is negative up to roughly 0.5λ, while the zero-crossing is always close to $s/\lambda = 1$. One furthermore finds a distinct quasi-linear increase with the separation arclength for all DNS cases beyond the minimum. The slope however, varies for the different flows. The deviations from the linear scaling for large separation distances $s > 3.5\lambda$ may be attributed to the small number of gradient trajectories

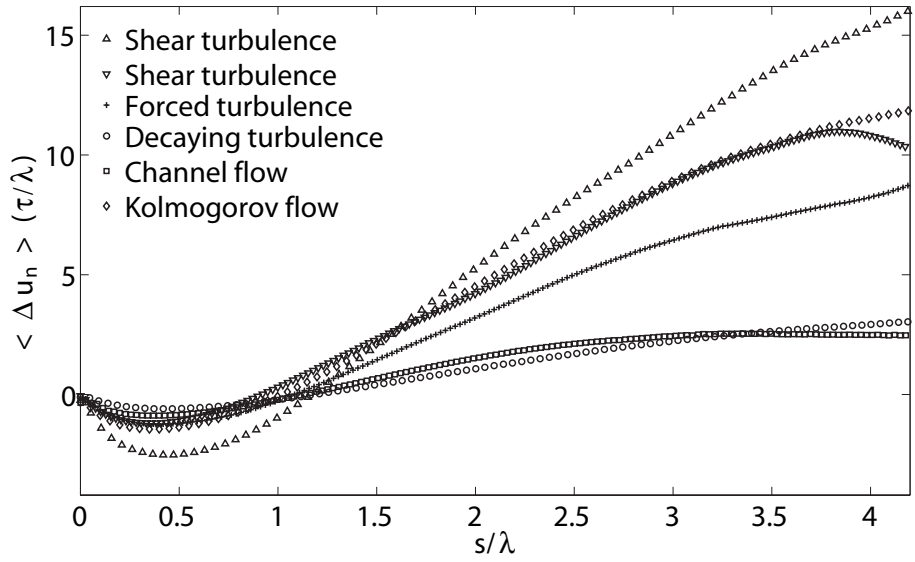

Figure 5. Non-dimensional first order velocity structure function $< \Delta u_n > \tau/\lambda$ along a gradient trajectory for cases 1-6.

of such a length, an obstacle which is overcome in the DNS of shear turbulence, which employs 2048^3 grid points, as in this case the increase is linear up to $s \approx 8\lambda$. As illustrated in figure 1 for the length distribution of dissipation elements, the majority of elements has a linear length of order λ. The probability to find an element longer than $s > 3.5\lambda$ is consequently very small. Even though for the conditioned mean velocity increment the curvilinear arclengths, which obviously is longer than the linear distance, is used, the difference between the linear distance of two extreme points and their curvilinear distance is relatively small. Summarizing, it can be concluded that while the linear increase of $< \Delta u_n >$ with s/λ in the inertial range can be considered as well established, the proportionality constant depends on the flow.

This is not surprising since $< \Delta u_n >$ is normalized in figure 5 with the integral time scale of the respective DNS case. On the other hand large dissipation elements are strained by a_∞ such that the projected velocity difference Δu_n at the extreme points of an element in direction of the linear connecting line is proportional to la_∞. Therefore, one may expect that the strain rate of individual trajectories within an element, especially for large separation distances s, will be exposed to the extensive strain a_∞.

To normalize the slope of the profile of $< \Delta u_n >$ for large s, we therefore propose to non-dimensionalize it by using the strain a_∞, rather than the integral time scale τ. This is shown in figure 6. Compared with figure 5, the new scaling $< \Delta u_n > /(a_\infty \lambda)$ naturally retains the zero-crossing at approximately $s = \lambda$, but in addition collapses the profiles so that the results of the different DNS cases now lie close to each other with a slope of approximately 0.5.

This normalization of $< \Delta u_n >$ using the strain rate a_∞ connects the two-point correlation along gradient trajectories with the concept of dissipation elements. Though all gradient trajectories connecting the same two extreme points are only described by the parameters of their dissipation element, this generalized three-dimensional information is still valid when returning to a one-dimensional trajectory.

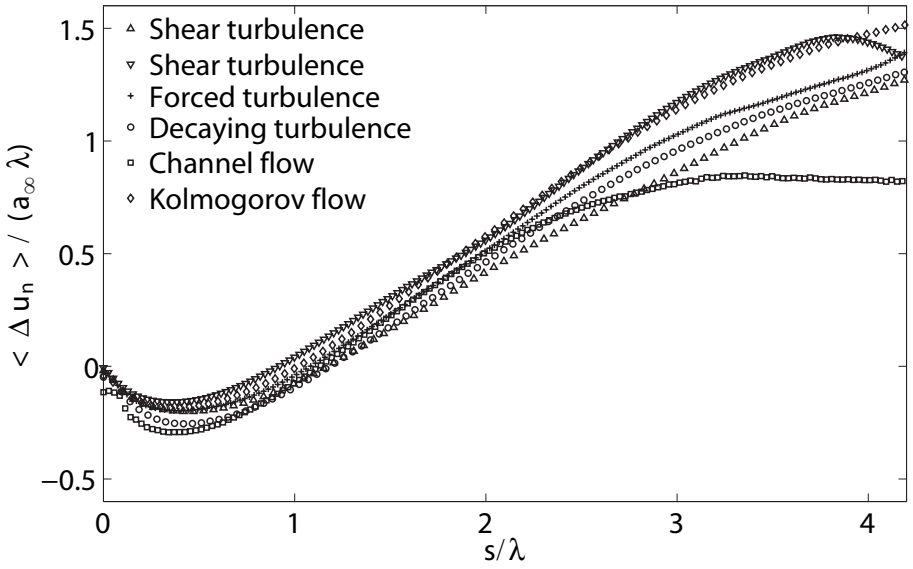

Figure 6. Non-dimensional first order velocity structure function $< \Delta u_n > /(a_\infty \lambda)$ along a gradient trajectory for DNS cases 1-6.

4. Conclusion

Dissipation element analysis based on the instantanous field of the kinetic energy has been extended from homogenous shear turbulence to different other types of turbulent flows exhibiting a wide range of Taylor based Reynolds numbers. For all cases the mean length of the dissipation elements was found to be of the order of the Taylor scale. The normalized pdf of the length of the dissipation elements was found to be Reynolds number independant, in agreement with the previous findings for homogenous shear turbulence. In addition, it was found that the flow configuration does not have a noticeable effect on the shapes of the normalized pdfs. This leads to the conclusion that the relevant physical effects which determine the pdf are independant of residual inhomogeneities or anisotropies. The model equation for the pdf was found to be in good agreement for all cases discussed. The first order structure function of the scalar difference at the ending points of the dissipation elements was found to scale approximately as $l^{2/3}$ in accordance with dimensional analysis. The velocity difference at the ending points however, revealed a linear scaling with the elements linear length for all DNS cases. This result was further analyzed in terms of the first order velocity structure function along gradient trajectories.

In a first step, Wang's scaling was examined for the different turbulent flows, which revealed a negative $< \Delta u_n > (\tau/\lambda)$ for small separation distance, followed by a linear increase with a zero-crossing around λ. As shown by Wang (2009), the slope of this linear scaling varies from case to case and is therefore not universal. In a second step however, $< \Delta u_n >$ was normalized by the asymptotic strain rate calculated for dissipation elements, as strain is the dominating physical mechanism acting on long gradient trajectories. The first order structure function along gradient trajectories normalized with the strain rate $< \Delta u_n > /(a_\infty \lambda)$ consequently exhibited the same shape for all turbulent flows. The successful normalization of statistics along gradient trajectories using the strain rate of dissipation elements in addition illustrated the physicly meaningful generelization used in dissipation element analysis.

Acknowledgments

This work has been funded by the Deutsche Forschungsgemeinschaft under grant Pe 241/30-3. Furthermore, the project has been continuously sponsored by NIC at the Research Center Juelich.

References

Gibson, C. H. 1968 Fine structure of scalar fields mixed by turbulence i. zero gradient points and minimal gradient surfaces. *Phys. Fluids* **11**, 2305–2315.

Schaefer, L., Dierksheide, U., Klaas, M. & Schroeder, W. 2010*a* Investigation of dissipation elements in a fully developed turbulent channel flow by tomographic particle-image velocimetry. *Phys. Fluids* **23**, 035106.

Schaefer, P., Gampert, M., Gauding, M., Peters, N. & Treviño, C. 2010*b* The secondary splitting of zero gradient points in a turbulent scalar field. *J. Eng. Math.* pp. DOI 10.1007/s10665–011–9452–x.

Schaefer, P., Gampert, M., Goebbert, J. H., Wang, L. & Peters, N. 2010*c* Testing of different model equations for the mean dissipation using Kolmogorov flows. *Flow, Turbulence and Combustion* pp. DOI 10.1007/s10494–010–9273–4.

Schaefer, P., Gampert, M., Wang, L. & Peters, N. 2009 Fast and slow changes of the length of gradient trajectories in homogenous shear turbulence. In *Advances in Turbulence XII* (ed. B. Eckhardt), pp. 565–572. Springer-Verlag, Berlin Heidelberg New York Tokyo.

Wang, L. 2009 Scaling of the two-point velocity difference along scalar gradient trajectories in fluid turbulence. *Phys. Rev.* **E 79, 046325**, 046325.

Wang, L. & Peters, N. 2006 The length scale distribution function of the distance between extremal points in passive scalar turbulence. *J. Fluid Mech.* **554**, 457–475.

Wang, L. & Peters, N. 2008 Length scale distribution functions and conditional means for various fields in turbulence. *J. Fluid Mech.* **608**, 113–138.

Wang, L. & Peters, N. 2011 The mean velocity increment conditioned on gradient trajectories of various scalar variables in turbulence. *accepted for publication in Phys. Scripta T* .